Enhancement of Conductivity by Diameter Control of Polyimide-Based Electrospun Carbon Nanofibers

ARTICLE *in* THE JOURNAL OF PHYSICAL CHEMISTRY B · NOVEMBER 2007

Impact Factor: 3.3 · DOI: 10.1021/jp075541q · Source: PubMed

THE JOURNAL OF PHYSICAL CHEMISTRY B LETTERS

2007, *111,* 11350−11353
Published on Web 09/13/2007

Enhancement of Conductivity by Diameter Control of Polyimide-Based Electrospun Carbon Nanofibers

Nguyen Thi Xuyen,[†] Eun Ju Ra,[†] Hong-Zhang Geng,[†] Ki Kang Kim,[†] Kay Hyeok An,[‡] and Young Hee Lee*,[†]

Department of Nanoscience and Nanotechnology, Department of Physics, Center for Nanotubes and Nanostructured Composites, Sungkyunkwan Advanced Institute of Nanotechnology, Sungkyunkwan University, Suwon, 440-746, South Korea, and R&D Department, Chonju Machinery Research Center, Chonju 561-844, South Korea

Received: July 16, 2007; In Final Form: August 26, 2007

Oxydianiline-pyromellitic dianhydride poly(amic acid) (ODA-PMDA PAA) was polymerized with a catalyst support of triethyl amine for controlling molecular weight. This polymer was used for electrospinning in the preparation of PAA nanofibers, a precursor of carbon nanofibers. Here the amount of catalyst and concentration of PAA solution were optimized to produce polyimide-based carbon nanofibers approximately 80 nm in diameter. The effects of molecular weight of PAA, bias voltage, and spinning rate on the morphology of electrospun PAA and polyimide nanofibers have been evaluated. We showed that the conductivity of the carbon nanofiber mat decreased with increasing nanofiber diameter, where the conductivity of polyimide-based carbon nanofiber mat was much higher than those of other types of carbon nanofiber mat. The key ingredient to increase conductivity in a carbon nanofiber mat was found to be the number of cross junctions between nanofibers.

Introduction

The choice of electrode material for electrochemical devices is an important factor affecting both performance and cost of the material.[1−6] In general, an electrode with good electrical conductivity and a large surface area is required for ideal performance of electrodes. Utilizing graphite powder,[7,8] cup-stacked-type carbon nanofibers,[9] vapor-grown carbon nanofibers,[10] carbon rods,[11] and similar materials requires the use of binders, which degrade the conductivity of electrodes. An electrospun carbon nanofiber mat appears to be a promising approach. The self-assembled nanofiber mat can, in principle, achieve a relatively high electrical conductivity by the binder-free process, and a large surface area is attainable because of the formation of small-diameter nanofibers in the mat.

Electrospinning has been used in the production of cellulos, polynos, nonoheterocyclic aromatic, linear thermoplastic, and heterocyclic polymers, but all have suffered from low carbonization yields.[12] Poly acrylonitrile (PAN) fibers, however, were carbonized with high yield commercially,[13] but its carbon fiber mat had limited conductivity (1.2 S cm^{-1}) that prevents it from widespread use as an electrode material. Recently, high-temperature-resistant organic polymers, (oxidianiline-pyromellitic dianhydride: ODA-PDMA) polyimide (PI) have been successfully electrospun and converted into carbon fibers of several micrometers in diameter with high carbonization yields.[14−17] This material showed an increase in electrical conductivity to 2.5 S cm^{-1}. Despite the possibility of conductivity improvement by diameter reduction, to our knowledge there has not been any research performed in this area.

In this work, we present a new strategy for accurate nanometer-scale diameter control of carbon fiber. This method is based on using a catalyst, triethyl amine (TEA), to control the molecular weight of the PAA polymer, a precursor of (ODA-PMDA) PI. Next, the effects of carbon nanofiber diameter and mat packing on its electrical conductivity were evaluated. The carbon nanofibers of 80-nm diameter reveal excellent electrical conductivity (16 S cm^{-1}); much higher than that of previous reports.[14,15−17]

Experimental Methods

Precursor Synthesis. The synthesis of conventional polyimide (PI) involved poly(amic acid) (PAA, Sigma Aldrich) formed from pyromellitic dianhydride (PMDA, Sigma Aldrich) and oxydianiline (ODA). Prior to use, both chemicals were dried in vacuum oven at room temperature. Next, 4 g of the monomer ODA was dissolved into 21 g of DMF solution (99.8 wt %). This solution was kept at ∼5 °C before use. PMDA (4.4 g) was added, and the mixture was stirred for 30 min using a magnetic bar. After which, the clear and viscous polymer solution was separated into four samples. Triethyl amine catalyst (TEA, Sigma Aldrich) with 0, 1, 3, and 5 wt % was then added into each sample to control the molecular weight. Note that for good mixing stirring was maintained by a mechanical stirrer until the entire quantity of TEA was added. The as-synthesized PAA was kept at −5 °C to maintain properties essential for further processing.

* Corresponding author. E-mail leeyoung@skku.edu.
[†] Sungkyunkwan University.
[‡] Chonju Machinery Research Center.

10.1021/jp075541q CCC: $37.00

Fabrication of ODA-PMDA PI-Based Carbon Nanofibers. The synthesized PAA solution with catalyst was electrospun into nanofibers onto a cylindrical collector wrapped in aluminum foil. The syringe was 2 cm in diameter and 10 cm long. The separation distance between the needle and collector was 15 cm. DC bias voltage and catalyst flow rates were optimized to stabilize the spinning jets in a room-temperature environment with ~30% humidity. The PAA nanofiber mat that was removed from the substrate was then converted into a polyimide nanofiber mat (PI) and stabilized by the optimum conditions. The procedure, which is composed of seven different oxidation steps at a rate of 1 °C/min, is described elsewhere.[18] Finally, a carbon nanofiber mat was formed by firing a PI nanofiber mat pressed between two plates of alumina under a 3-sccm argon gas flow at 1000 °C. This occurred in three steps: from room temperature to 600 °C in 1 h, from 600 to 1000 °C in 1.3 h, and 1000 °C maintained for 1 h. (See Supporting Information S1 for the structural transformation.)

Measurements. The molecular weight of PAA in DMF solvent was measured by gel permeation chromatography (GPC). The sheet resistance (R_s) was measured using the four-point probe method (Keithley 2000 multimeter) at room temperature. R_s was calculated using the equation $R_s = 4.532R$ and the resistivity $\rho = 4.532tR$, where $R = V/I$ and t is the thickness of the sample. Field-emission scanning electron microscopy (FESEM: JEOL 6700F) was also used to characterize the morphology of the nanofibers. Nanofiber diameter estimation was done by measuring the diameter of about 30 different fibers and taking the average.

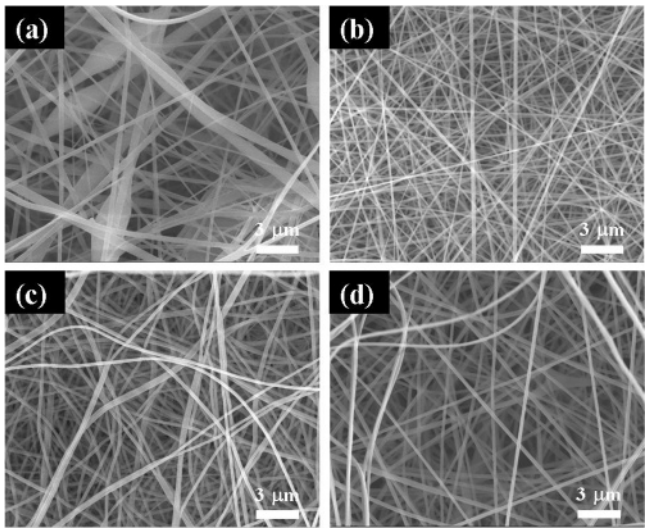

Figure 1. Morphology of electrospun (ODA-PMDA) PAA nanofibers of 20 wt % PAA at (a) 0 wt %, (b) 1 wt %, (c) 3 wt %, and (d) 5 wt % catalyst TEA.

Results and Discussion

Molecular Weight Dependence of the Diameter. Figure 1 presents the FE-SEM images of the electrospun nanofiber mats with respect to catalyst content. These samples were obtained by optimizing the bias voltage and flow rate during electrospinning. For example, in the case of no catalyst, it was difficult to obtain the small-diameter nanofibers without bead formation. There was also a wide diameter distribution in this situation. However, in the presence of catalyst, no bead formation was observed. There was a very uniform diameter distribution, and the average diameter showed a strong correlation to the catalyst content. It has been suggested that the addition of TEA catalyst into the PAA solution improves polymer properties, where the TEA catalyst helps connect reactive excess monomers with short polymer chains. As a consequence, the obtained PAA solution had not only longer polymer chains but also a very narrow length distribution. These statements were verified by the existence of one sharp peak in the GPC data (not shown here).

Figure 2a presents the mean diameter of PAA nanofibers as a function of catalyst content. With small molecular weight in the absence of catalyst, entanglements among polymer chains became poor. Thus, the discontinuous jets were favorably formed under static electrical force. The PAA solution was then likely to be sprayed rather than electrospinning. The electrospinning was realized with slightly modified electrospraying conditions. As a consequence, some beads were formed, revealing a wide diameter distribution with a large fluctuation in mean diameter, as illustrated in Figure 1a. By introducing a small amount of catalyst with 1 wt % of TEA, the degree of entanglement was improved significantly and the electrospinning produced small-diameter fibers without any beads. By adding more catalyst, the solution showed increased viscosity with very densely entangled polymer chains. The chains were entangled so densely that that the stretching of polymer jets was difficult to achieve using electrostatic force even with a high critical voltage. As a consequence, the diameter of the nanofibers increased as well as the diameter variability.

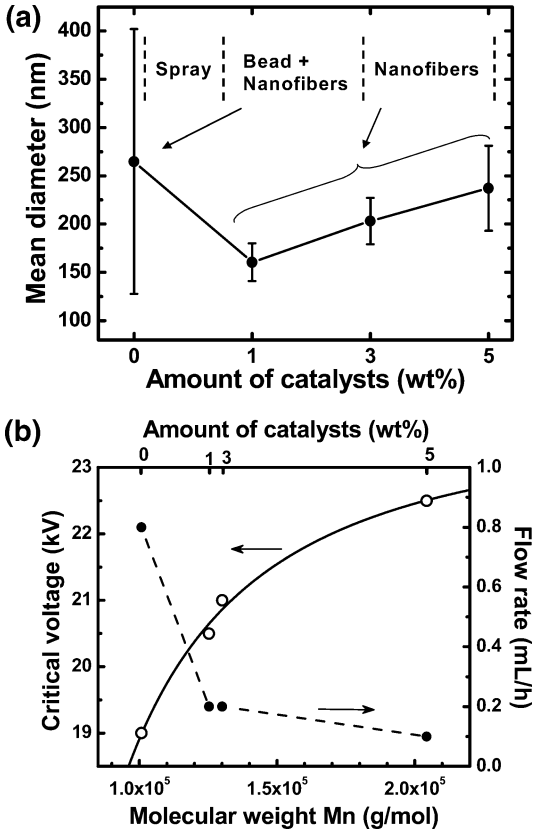

Figure 2. (a) Mean diameters of (ODA-PMDA) PAA nanofibers as a function of the amount of TEA catalyst. (b) Electrospinning conditions involved critical voltage (blank circle) and flow rate (solid circle) of (ODA-PMDA) PAA solution as a function of its molecular weight.

Electrospinning Processing. To optimize the electrospinning parameters, we held constant the separation distance, the winding speed of drum cathode, and solution concentration. The dc bias voltage and flow rate were varied to find the best condition. The molecular weight increased generally with

increasing catalyst content, as can be seen in Figure 2b. With increasing molecular weight, the degree of entanglement of the polymer chains increases as well. The stable jet ejected from Taylor's cone is subject to larger tensile stresses and may undergo significant flow elongation. The formation of a Talor cone at the tip of a needle requires high bias. Here, we defined a critical voltage to maintain the Taylor cone and stabilized the electrospinning for a long enough time to fabricate a mat thick enough (more than 300 μm) to serve as an electrode for several applications. A balance for the flow rate had to be kept both to prevent the formation of droplets at the tip of a needle and to continue the electrospinning. This critical voltage increases rapidly initially and then saturates at high molecular weight limit, exhibiting quadratic behavior. It has been reported in the literature that the surface tension shows a quadratic behavior with molecular weight.[19] Moreover, the critical field is related to the surface tension.[20] Thus, we expect the critical field to berelated to the polymer molecular weight according to the following equation

$$E_{\text{critical}}{}^2 \simeq 563\left[1 - \left(\frac{57\,178}{M_n}\right)^{1.8}\right]$$

where E_{critical} is the critical voltage and M_n is a molecular weight of the ODA-PMDA PAA polymer. The fitted curve represents the data points well. The critical exponent is 1.8 in our case. The exponents of $^2/_3$ and 1 represent two limits of low and medium molecular weight, respectively, and have been proven experimentally as well.[19,21] It has been predicted that the exponent of 2 satisfies the limit of high molecular weight, although no experimental evidence was provided for this. For our case, we believe that the critical exponent of 1.8 represents the limit of high-molecular-weight polyimide. The minimum molecular weight was 0.57×10^5 g/mol, and the maximum critical voltage was about 24 kV. It is worth noting that the polymer solution concentration influenced significantly the surface tension at low molecular weight.[22] However, at high molecular weight, the polymer solution concentration did not appreciably influence the surface tension, in agreement with the literature. The flow rate is another important parameter to stabilize electrospinning. In general, the flow rate can be kept constant by changing the critical voltage, that is, by increasing the critical voltage with increasing molecular weight. However, in our case the molecular weight was large enough that the flow rate as well as the critical voltage changed to ensure stable electrospinning.

PAA Concentration Dependence of the Diameter. Figure 3 shows the minimum mean diameter of PAA nanofiber of 157 nm at a PAA concentration of 20 wt % with a catalyst content of 1 wt %. We chose this condition and tried to optimize the diameter of PAA nanofibers by varying the PAA concentration. In general, the nanofiber diameter can be altered with solution concentration. For a given PAA concentration in DMF solution, the voltage and flow rate were again controlled to maintain the stable electrospinning process. All other parameters were kept unchanged At a concentration of 1 wt % of catalyst, the voltage increased slightly from 20.3 to 20.6 kV, when the PAA concentration changed from 18 to 20 wt % because of the high molecular weight of the polymer. The mean diameter of the PAA nanofibers increased with a power law for high PAA concentrations. This trend was similar to previous work performed on many other kinds of polymers.[23−25] What is more intriguing is that the mean diameter increased again at the low PAA concentration limit. Consequently, the minimum position in the diameter was observed and is shown in Figure 2a. We note that at a PAA concentration of 17 wt % some beads were formed. This phenomenon is similar to the bead formation without catalyst at a PAA concentration of 20 wt %, where a large mean diameter of 260 nm was obtained. This is another case where the elastic of the jet decreased so that the jet's elongation could no longer remain continuous, reaching the so-called "spray-spin transition" region.

Using the stabilization and carbonization described in the Experimental Section, we experienced a similar trend for diameter variation. The diameter decreased with a similar trend, independent of PAA concentration. The as-synthesized electrospun nanofiber mat contained solvent and catalyst that may have remained from electrospinning. These were removed during stabilization, and, more importantly, the hydrative cycloimidization occurs to transform to PI nanofibers. Carbonization involves removal of the heteroatom and cross-linking of the molecular chain to transform into graphene layers. Thus, some amount of weight loss is expected during carbonization. A diameter reduction rate of only about 15% was observed during this process, a value much smaller than that for large-diameter nanofibers (about 50%). The yield of carbonization of our small-diameter nanofiber mat was 57 wt %, slightly larger than that of large-diameter nanofiber mat.[14,15] We emphasize that a diameter of 80 nm was obtained with our current optimization process. However, we believe there is still room to improve the electrospinnning conditions, perhaps with more catalyst content and lower PAA concentration that may result in diameters smaller than 80 nm.

Electrical Conductivity of Carbon Nanofiber Mat. Figure 4 shows the conductivity that strongly depended on the pressure applied during carbonization, as well as on the mean diameter of the carbon nanofibers. At zero pressure and without an

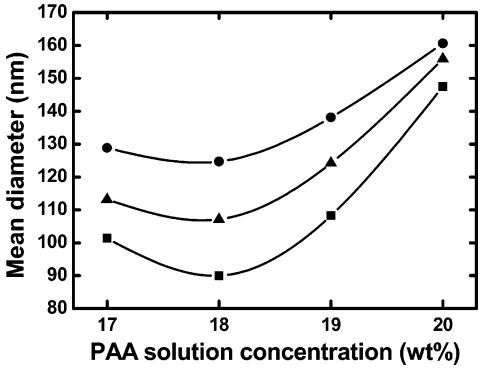

Figure 3. Mean diameters of (ODA-PMDA) PAA (circle), (ODA-PMDA) PI (triangle), and carbon (square) nanofibers as a function of PAA concentration at 1 wt % TEA catalyst.

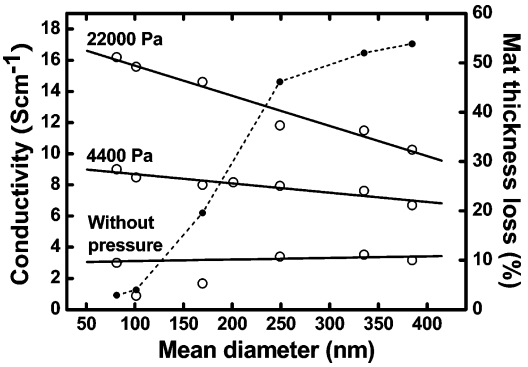

Figure 4. Conductivity of carbon nanofiber mats (solid line) and mat thickness loss, which was compared between two cases at 4400 and 22000 Pa (dashed line) as a function of diameter of carbon nanofibers.

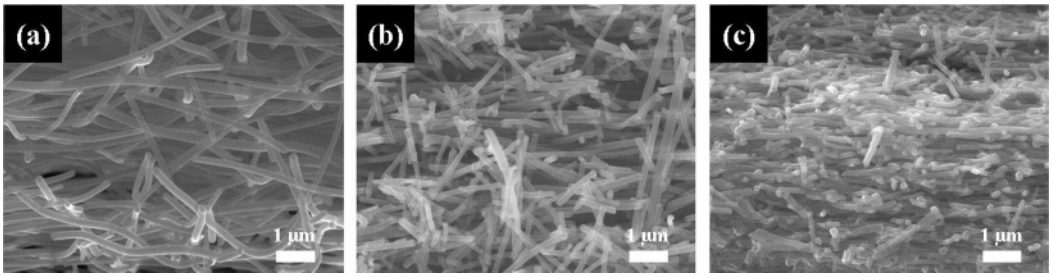

Figure 5. SEM cross-section images of carbon nanofiber (a) without pressure, (b) with pressure of 4400 Pa, and (c) with 22 000 Pa applied on (ODA-PMDA) the PI nanofiber mat during the carbonization process.

alumina plate on top of the mat during carbonization, the conductivity remained almost constant and independent of the mean diameter. On the other hand, with increasing pressure, the conductivity was enhanced prominently. The conductivity increased with decreasing diameter. As the pressure was increased, this diameter dependence of conductivity became increasingly more prominent. Interestingly, the thickness of the mat was reduced significantly more for larger diameters, as indicated by the short-dashed line in Figure 4. This densification can be seen in the SEM images of the cross section in Figure 5. Moreover, as observed by top-view SEM, the morphology of carbon nanofiber mats did not change (broke or fractured) for pressures up to 22 000 Pa. For a nanofiber mat with diameter of 80 nm, the conductivity was 16 S/cm, exceeding the value (2.5 S/cm) of a PI-based carbon nanofiber mat with a diameter of 1−2 μm fabricated under the same carbonization conditions.[13,18] This value is also much higher than that (1.2 S/cm) of a PAN-based carbon nanofiber mat.

The equivalent resistance of the nanofiber mat is a sum of the resistance of nanofibers and the contact resistance of cross junctions between nanofibers. Consequently, the conductivity of the carbon nanofiber mat may depend on the packing density of nanofibers and diameter of nanofibers, both of which affect the numbers of cross junctions between nanofibers per unit volume of the mat. If one were to presume that the conductivity depends only on the packing density, then the packing density would increase at higher pressure. This would continue until eventually complete contacts between the nanofibers were formed. In the case of equal numbers of cross junctions, there should be no diameter dependence of conductivity. However, we observed a very strong dependence with increasing pressure. This indicates that the number of cross junctions increased with decreasing diameters. High-density nanofibers with small diameters seemed to provide a large number of cross junctions. As a consequence, the conductivity was enhanced at high packing density and for a small-diameter nanofiber mat.

Conclusions

TEA catalyst has been used to enhance the molecular weight of polymerization PAA in DMF. Using electrospinning, the diameter of PAA nanofibers was controlled by varying the molecular weight of PAA and concentration of PAA/DMF solutions. The relationship between critical voltage and molecular weight obtained was in excellent agreement with a theoretical model at the limit of high molecular weight. At the optimal conditions for imidization and carbonization processes, the diameters of PAA fibers reached a minimum value of around 80 nm. We also observed an increased conductivity of the nanofiber mat with increased packing density and smaller diameter because of more cross junctions between nanofibers.

Acknowledgment. This work was financially supported by STAR-faculty project from MOE and in part by the KOSEF through CNNC at SKKU, and MOE, MOCIE, and MOLAB through the foresting project of laboratory of excellence. I thank Nguyen Thanh Tien for useful discussions.

Supporting Information Available: FTIR spectra. This material is available free of charge via the Internet at http://pubs.acs.org.

References and Notes

(1) Winter, M.; Brodd, R. *Chem. Rev.* **2004**, *104*, 4245.
(2) Li, D.; Xia, Y. *Adv. Mater.* **2004**, *16*, 1151.
(3) Marsh, H.; Heintz, E. A.; Reinoso, F. R. *Introduction to Carbon Technology*; Universidal de Alicante, Secretariadode Publications: Alicante, Spain, 1997.
(4) Wang, H.; Abe, T.; Maruyama, S.; Iriyama, Y.; Ogumi, Z.; Yoshikawa, K. *Adv. Mater.* **2005**, *17*, 2857.
(5) Fletcher, B. L.; McKnight, T. E.; Melechko, A. V.; Hensley, D. K.; Thomas, D. K.; Ericson, M. N.; Simpson, M. L. *Adv. Mater.* **2006**, *18*, 1689.
(6) Guha, A.; Lu, W.; Zawodzinski, T. A., Jr.; Schiraldi, D. A. *Carbon* **2007**, *45*, 1506.
(7) Xi, J.; Wang, J.; Yu, L.; Qiu, X.; Chen, L. *Chem. Commun.* **2007**, *16*, 1656.
(8) Rabinovich, L.; Gun, J.; Lev, O.; Aurbach, D.; Markovsky, B.; Levi, M. D. *Adv. Mater.* **1998**, *10*, 157.
(9) Endo, M.; Kim, Y. A.; Ezaka, M.; Osada, K.; Yanagisawa, T.; Hayashi, T.; Terrones, M.; Dresselhaus, M. S. *Nano Lett.* **2003**, *3*, 723.
(10) Guo, J.; Sun, G.; Wang, Q.; Wang, G.; Zhou, Z.; Tang, S.; Jiang, L.; Zhou, B.; Xin, Q. *Carbon* **2006**, *44*, 152.
(11) Bose, A. B.; Sarkar, M.; Bose, R. N. *J. Power Sources* **2006**, *157*, 188.
(12) Chan, S. *J. Mater. Sci.* **2000**, *35*, 1303.
(13) Donnet, J. B.; Wang, T. K.; Peng, J. C. M.; Rebouillat, S. *Carbon Fibers*; DuPont de Nemours International S.A., Geneva, Switzerland, Marcek Dekker, Inc.: New York, 1998.
(14) Yang, K. S.; Edie, D. D.; Lim, D. Y.; Kim, Y. M.; Choi, Y. O. *Carbon* **2003**, *41*, 2039.
(15) Kim, C.; Choi, Y. O.; Lee, W. J.; Yang, K. S. *Electrochim. Acta* **2004**, *50*, 883.
(16) Jang, J.; Lee, K. J.; Kim, Y. G. *Chem. Commun.* **2005**, *30*, 3847.
(17) Nah, C.; Han, S. H.; Lee, M. H.; Kim, J. S.; Lee, D. S. *Polym. Int.* **2003**, *52*, 429.
(18) Macossay, J.; Leal, J. H.; Kuang, A.; Jones, R. E. *Polym. Adv. Technol.* **2006**, *17*, 391.
(19) Jones, R. L.; Richards, R. W. *Polymers at Surface and Interfaces*; Cambridge University Press: Cambridge, 1999.
(20) Taylor, G. I. *Proc. R. Soc. London, Ser. A* **1969**, *313*, 453.
(21) Legrand, D. G.; Gaines, G. L., Jr. *J. Colloid Interface Sci.* **1969**, *31*, 162.
(22) Cao, B. H.; Kim, M. W. *Faraday Discuss* **1994**, *98*, 245.
(23) Yang, Q.; Li, Z.; Hong, Y.; Zhao, Y.; Qiu, S.; Wang, C.; Wei, Y. *J. Polym. Sci., Part B: Polym. Phys.* **2004**, *42*, 3721.
(24) Yang, Q.; Li, Z.; Hong, Y.; Zhao, Y.; Qiu, S.; Wang, C.; Wei, Y. *J. Polym. Sci., Part B: Polym. Phys.* **2004**, *42*, 372.
(25) Ryu, Y. J.; Kim, H. Y.; Lee, K. H.; Park, H. C.; Lee, D. R. *Eur. Polym. J.* **2003**, *39*, 1883.